

# Synthesis, spectroscopic and redox properties of the mononuclear Ni<sup>II</sup>, Ni<sup>II</sup>(BPh<sub>2</sub>)<sub>2</sub> containing (B–C) bond and trinuclear Cu<sup>II</sup>–Ni<sup>II</sup>–Cu<sup>II</sup> type-metal complexes of *N,N'*-(4-amino-1-benzyl piperidine)-glyoxime

AHMET KILIC<sup>a,\*</sup>, ESREF TAS<sup>a</sup> and ISMAIL YILMAZ<sup>b</sup>

<sup>a</sup>Department of Chemistry, University of Harran, Osmanbey Campus, 63190 Sanliurfa, Turkey

<sup>b</sup>Department of Chemistry, Technical University of Istanbul, 34469, Istanbul, Turkey

e-mail: kilica63@harran.edu.tr

MS received 7 March 2008; revised 11 November 2008

**Abstract.** The novel *vic*-dioxime ligand containing the 4-amino-1-benzyl piperidine group, *N,N'*-(4-amino-1-benzyl piperidine)-glyoxime, (LH<sub>2</sub>) has been prepared from 4-amino-1-benzyl piperidine with *anti*-dichloroglyoxime at –15°C in absolute THF. Mononuclear Ni<sup>II</sup> metal complex has been obtained with 1 : 2 metal/ligand ratio. The Ni<sup>II</sup> complex of this ligand is proposed to be square planar geometry. IR spectra show that the ligand acts in a tetradentate manner and coordinates N<sub>4</sub> donor groups of LH<sub>2</sub> to Ni<sup>II</sup> ion. The detection of H-bonding (O–H···O) in the [Ni(LH)<sub>2</sub>] (1) metal complex by IR spectra supported the square-planar MN<sub>4</sub> coordination of mononuclear complex. The disappearance of H-bonding (O–H···O) in the [Ni(L)<sub>2</sub>(BPh<sub>2</sub>)<sub>2</sub>] (2) complex shows that the BPh<sub>2</sub><sup>+</sup>-capped groups (BPh<sub>2</sub><sup>+</sup> cation formed BPh<sub>4</sub><sup>–</sup> anion) attaches to the main oxime core. MN<sub>4</sub> coordination of the [Ni(LH)<sub>2</sub>] (1) and [Ni(L)<sub>2</sub>(BPh<sub>2</sub>)<sub>2</sub>] (2) metal complexes were also determined by <sup>1</sup>H-NMR spectroscopy. In the trinuclear Cu<sup>II</sup>–Ni<sup>II</sup>–Cu<sup>II</sup> metal complexes, the Ni<sup>II</sup> ion centered into the main oxime core by the coordination of the imino groups while the two Cu<sup>II</sup> ions coordinate dianionic oxygen donors of the oxime groups and linked to the ligands of 1,10-phenanthroline, 2,2'-bipyridine, and 4,4'-bipyridine. The ligand and their mono and trinuclear metal complexes were characterized by elemental analyses, FT-IR, UV-Vis, <sup>1</sup>H and <sup>13</sup>C-NMR spectra, magnetic susceptibility measurements, molar conductivity, cyclic voltammetry, mass spectra and X-ray powder techniques. The cyclic voltammetric results show that the cathodic peak potential of [Ni(L)<sub>2</sub>(BPh<sub>2</sub>)<sub>2</sub>] shifted toward more negative value compared to that of [Ni(LH)<sub>2</sub>], probably due to a decreasing effect of back donation of metal-oxime moieties as a result of the BPh<sub>2</sub><sup>+</sup>-bridged complex formation. Also, the formation of the trinuclear Cu<sup>II</sup>–Ni<sup>II</sup>–Cu<sup>II</sup> metal complexes caused considerable changes on the CV behaviour of mononuclear [Ni(LH)<sub>2</sub>] (1) complex. The spectroelectrochemical study of [Ni(L)<sub>2</sub>(BPh<sub>2</sub>)<sub>2</sub>] (2) showed distinctive spectral changes that the intensity of the band (λ = at 364 nm, assigned to *n* → π\* transitions) decreased and a new broad band in low intensity about 460 nm appeared as a result of the reduction of the nickel centered in the oxime core.

**Keywords.** *vic*-dioxime; synthesis; spectroscopy; electrochemistry; spectroelectrochemistry.

## 1. Introduction

The study of the coordination of transition metal ions to different types of ligands has been amplified by the recent developments in the fields of bioinorganic chemistry and medicine. Whereas the knowledge of coordination chemistry is essential to the understanding of the structural and functional features of metalloproteins, its medical application ranges from the development of MRI contrasting agents, radiopharmaceuticals, chemotherapeutics to

the treatment of metal toxicity.<sup>1</sup> The synthesis of *vic*-dioximes and their different derivatives have been the subject of study for very long period. The transition metal complexes of *vic*-dioximes have been of particular interest as biological model compounds.<sup>2</sup> Moreover, *vic*-dioximes are interesting for many applications in a variety of high technology fields, such as medicine,<sup>3–5</sup> catalysis,<sup>6,7</sup> electro optical sensors,<sup>8</sup> liquid crystals,<sup>9</sup> and trace metal analysis.<sup>10</sup> Interest in the metal coordination environment has prompted the study of oxime ligands due to their variable geometries<sup>2</sup> and the tunability of their substituents.<sup>11,12</sup> The biological activities of Ni<sup>II</sup>, Ph<sub>2</sub>B–Ni<sup>II</sup>–BPh<sub>2</sub> and Cu<sup>II</sup>–Ni<sup>II</sup>–Cu<sup>II</sup> metal complexes can

\*For correspondence

be increased when mixed-ligand complexes with heterocyclic bases, such as 1,10-phenanthroline, 2,2'-bipyridine, 4,4'-bipyridine, pyridine, and  $\text{BPh}_2^+$  are involved. For example, trinuclear  $\text{Cu}^{\text{II}}-\text{Ni}^{\text{II}}-\text{Cu}^{\text{II}}$  complexes having a ligand with nitrogens and oxygens donor atoms show DNA binding and antitumor activity.<sup>13</sup> The tetradentate *vic*-dioxime ligands behave similarly by enveloping themselves around metal ions in a planar geometry, forming a hydrogen bond between the two oxime groups by removing one hydrogen ion. The strength of the hydrogen bond between the two oxime groups, which is represented by the O–O distance, is dependent on the size of the metal ions and chemical environment around the metal ions. Accordingly, the position of the hydrogen bonded-oxime proton in the  $^1\text{H-NMR}$  spectrum can be correlated with the strength of the hydrogen bond.<sup>14</sup> The ability of donor atoms to stabilize reduced and/or oxidized forms of metal has sparked interest in their role in bioinorganic systems. So, for a better understanding of their properties, the investigation of redox behaviour has a vital importance. Although various *vic*-dioximes and their metal and non-metal compounds have been studied extensively, redox properties of *vic*-dioximes is scarce.<sup>15</sup>

In the present work, we have prepared a new *vic*-dioxime ligand and its mononuclear  $\text{Ni}^{\text{II}}$ ,  $\text{Ni}^{\text{II}}(\text{BPh}_2)_2$  and trinuclear  $\text{Cu}^{\text{II}}-\text{Ni}^{\text{II}}-\text{Cu}^{\text{II}}$  metal complexes. Synthesis, characterization, spectroscopic, and electrochemical properties of the new *vic*-dioxime metal complexes have been investigated in detail. The ligand and complexes have been identified by a combination of elemental analyses,  $^1\text{H-NMR}$  and  $^{13}\text{C-NMR}$  spectra, FT-IR spectra, UV-Vis spectra, magnetic susceptibility measurements, X-ray powder diffraction measurements, molar conductivity measurements and cyclic voltammetric measurements. The first aim of this study is to prepare a new highly soluble trinuclear *vic*-dioxime complex  $[\text{Ni}(\text{L})_2(\text{BPh}_2)_2]$  (**2**),  $[\text{Ni}(\text{L})_2\text{Cu}_2(1,10\text{-phen})_2](\text{ClO}_4)_2$  (**3**),  $[\text{Ni}(\text{L})_2\text{Cu}_2(2,2'\text{-bpy})_2](\text{ClO}_4)_2$  (**4**), and  $[\text{Ni}(\text{L})_2\text{Cu}_2(4,4'\text{-bpy})_2(\text{H}_2\text{O})_2](\text{ClO}_4)_2$  (**5**) metal complexes. The second aim is to compare their electrochemical behaviour to understand the effect of the coordination of the  $\text{BPh}_2^+$ -capped ion or bidentate ligands such as 1,10-phenanthroline, 2,2'-bipyridine, and 4,4'-bipyridine to the oxime moieties through two oxygen donor atoms. Third aim is to understand their crystalline or amorphous structures by X-ray powder analysis as well.

## 2. Experimental

All reagents and solvents were of reagent grade quality and obtained from commercial suppliers (Fluka Chemical Company, Taufkirchen, Germany). Tetra-*n*-butylammonium perchlorate (TBAP, Fluka) was used as received. (*E,E*)-dichloroglyoxime was prepared by a reported procedure.<sup>16,17</sup> The elemental analyses were carried out in the Laboratory of the Scientific and Technical Research Council of Turkey (TUBITAK). IR spectra were recorded on a Perkin Elmer Spectrum RXI FT-IR Spectrometer as KBr pellets.  $^1\text{H-NMR}$  and  $^{13}\text{C-NMR}$  spectra were recorded on a Bruker-Avence 400 MHz spectrometers. Magnetic Susceptibilities were determined (table 1) on a Sherwood Scientific Magnetic Susceptibility Balance (Model MK1) at room temperature (20°C) using  $\text{Hg}[\text{Co}(\text{SCN})_4]$  as a calibrant; diamagnetic corrections were calculated from Pascal's constants.<sup>18</sup> UV-Vis spectra were recorded on a Shimadzu 1601 PC. Molar conductivities ( $\Lambda_{\text{M}}$ ) were recorded on a Inolab Terminal 740 WTW Series. MS results were recorded on a Micromass Quattro LC/ULTIMA LC-MS/MS spectrometer. X-ray powder were recorded on a Rigaku Ultima III Series. Cyclic voltammograms (CV) were carried out using CV measurements with Princeton Applied Research Model 2263 potentiostat controlled by an external PC. A three electrode system (BAS model solid cell stand) was used for CV measurements in DMSO and consisted of a 2 mm sized platinum disc electrode as working electrode, a platinum wire counter electrode, and an Ag/AgCl reference electrode. The reference electrode was separated from the bulk solution by a fritted-glass bridge filled with the solvent/supporting electrolyte mixture. The ferrocene/ferrocenium couple ( $\text{Fc}/\text{Fc}^+$ ) was used as an internal standard but all potentials in the paper are referenced to the Ag/AgCl reference electrode. Solutions containing complexes were deoxygenated by a stream of high purity nitrogen for at least 5 min. Before running the experiment and the solution was protected from air by a blanket of nitrogen during the experiment. Controlled potential electrolysis (CPE) was performed with Princeton Applied Research Model 2263 potentiostat/Galvanostat. An BAS model electrolysis cell with a fritted glass to separate the cathodic and anodic portions of the cell was used for bulk electrolysis. The sample and solvent were placed into the electrolysis cell under nitrogen.

### 2.1 Synthesis of the ligand (LH<sub>2</sub>)

2.50 g, 16 mmol of 4-Amino-1-benzyl piperidine was dissolved in 70 cm<sup>3</sup> absolute THF. Then, 3.23 g, 32 mmol triethylamine (Et<sub>3</sub>N) was added and the mixture was cooled to -15°C and kept at this temperature. To this solution, 6.10 g, 32 mmol *anti*-dichloroglyoxime in 50 cm<sup>3</sup> absolute THF was added drop-wise under a N<sub>2</sub> atmosphere with continuous stirring. The addition of the *anti*-dichloroglyoxime solutions was carried out during 4 h. The mixture was stirred for more than 3 h and the temperature was raised to 20°C. Precipitated Et<sub>3</sub>NHCl was filtered off and the filtrate was evaporated to remove THF. The oily products were dissolved in CH<sub>2</sub>Cl<sub>2</sub> (15 cm<sup>3</sup>) and n-hexane (100 cm<sup>3</sup>) added to precipitate the compounds. This process was then repeated several times. Ligand (LH<sub>2</sub>) were filtered and dried in a vacuum at 35°C. Ligand (LH<sub>2</sub>) are soluble in common organic solvents such as THF, EtOH, DMF and DMSO. IR (KBr pellets,  $\nu_{\max}/\text{cm}^{-1}$ ): 3617–3143  $\nu(\text{OH/NH})$ , 3028  $\nu(\text{Ar-H})$ , 2941, 2765  $\nu(\text{Aliph-H})$ , 1638  $\nu(\text{C=N})$ , 1367 and 983  $\nu(\text{N-O})$ . <sup>1</sup>H-NMR (CDCl<sub>3</sub>, TMS,  $\delta$  ppm): 9.56 (s, 2H, OH), 7.31–7.26 (m, 10H, Ar-CH), 5.15–5.13 (d, 2H, NH,  $J = 8$  Hz), 3.50 (s, 4H, N-<sup>5</sup>CH<sub>2</sub>), 2.82–2.80 (d, 2H,  $J = 8$ , N-CH), 2.07–2.01 (m, 8H, N-<sup>6</sup>CH<sub>2</sub>), 1.85–1.83 (d, 4H, C-CH<sub>2</sub>,  $J = 8$  Hz) and 1.60–1.55 (m, 4H, C-<sup>7</sup>CH<sub>2</sub>). <sup>13</sup>C-NMR (CDCl<sub>3</sub>, TMS,  $\delta$  ppm): C<sub>1</sub> (127.25), C<sub>2</sub> (128.27), C<sub>3</sub> (129.57), C<sub>4</sub> (137.42), C<sub>5</sub> (62.97), C<sub>6</sub> (52.23), C<sub>7</sub> (34.70), C<sub>8</sub> (49.99) and C<sub>9</sub> (147.65).

### 2.2 Synthesis of the metal complex [Ni(LH)<sub>2</sub>] (I)

A solution of nickel(II) chloride hexahydrate (0.26 g, 1.10 mmol) in absolute ethanol (50 cm<sup>3</sup>) was added to a solution of ligand (LH<sub>2</sub>) (1.0 g, 2.2 mmol), in absolute ethanol (75 cm<sup>3</sup>) at 55–60°C. A distinct change was observed in colour from colourless to red under a N<sub>2</sub> atmosphere with continuous stirring. Then, a decrease in the pH of the solution was observed. The pH of the solution was *ca.* 1.5–3.0 and was adjusted to 4.5–5.5 by the addition of a 1% triethylamine solution in EtOH. After heating the mixture for 4 h in a water bath, the precipitate was filtered off, washed with H<sub>2</sub>O and diethyl ether several times, and dried *in vacuo* at 35°C. IR (KBr pellets,  $\nu_{\max}/\text{cm}^{-1}$ ): 3336  $\nu(\text{NH})$ , 3026  $\nu(\text{Ar-H})$ , 2936, 2791  $\nu(\text{Aliph-H})$ , 1726  $\nu(\text{O-H}\cdots\text{O})$ , 1599  $\nu(\text{C=N})$ , 1366  $\nu(\text{N-O})$ . <sup>1</sup>H-NMR

(CDCl<sub>3</sub>, TMS,  $\delta$  ppm)  $\delta$ : 16.49 (s, 2H, O-H $\cdots$ O), 7.33–7.28 (m, 20H, Ar-CH), 4.80–4.77 (d, 4H, NH,  $J = 12$  Hz), 3.50 (s, 8H, N-<sup>5</sup>CH<sub>2</sub>), 2.85–2.82 (d, 4H, N-CH,  $J = 12$ ), 2.09–2.04 (t, 16H, N-<sup>6</sup>CH<sub>2</sub>,  $J = 20$ ), 1.91–1.88 (d, 8H, C-<sup>7</sup>CH<sub>2</sub>,  $J = 12$ ) and 1.55–1.53 (m, 8H, C-CH<sub>2</sub>). <sup>13</sup>C-NMR (CDCl<sub>3</sub>, TMS,  $\delta$  ppm): C<sub>1</sub> (127.08), C<sub>2</sub> (128.25), C<sub>3</sub> (129.00), C<sub>4</sub> (138.31), C<sub>5</sub> (62.86), C<sub>6</sub> (53.82), C<sub>7</sub> (33.99), C<sub>8</sub> (52.07) and C<sub>9</sub> (146.13).

### 2.3 Synthesis of the metal complex [Ni(L)<sub>2</sub>(BPh<sub>2</sub>)<sub>2</sub>] (2)

To a solution of ligand (LH<sub>2</sub>) (0.5 g, 1.0 mmol) in 125 ml of warm absolute ethanol (55–60°C) was added a solution of nickel(II) chloride hexahydrate (0.13 g, 0.50 mmol) in 20 ml of warm absolute ethanol (55–60°C) with stirring. The colour of the solution turned to red and then the ethanol solution was cooled to room temperature. A solution of excess NaBPh<sub>4</sub> (3.76 g, 11.0 mmol) in 45 ml absolute ethanol was added drop-wise to this clear red solution. A distinct change was observed in colour from red to orange under a N<sub>2</sub> atmosphere with continuous stirring. Then the ethanol removed under reduced pressure. The orange solid compound was dissolved with CH<sub>2</sub>Cl<sub>2</sub> (90 ml). The solution was filtered, extracted with water and then filtered. Removal of CH<sub>2</sub>Cl<sub>2</sub> gave an orange solid which was recrystallized from CH<sub>2</sub>Cl<sub>2</sub>/EtOH (1 : 8) to give orange crystals which were filtered, washed with EtOH, diethylether and dried. IR (KBr pellets,  $\nu_{\max}/\text{cm}^{-1}$ ): 3336  $\nu(\text{NH})$ , 3064–3024  $\nu(\text{Ar-H})$ , 2927–2770  $\nu(\text{Aliph-H})$ , 1616  $\nu(\text{C=N})$ , 1195  $\nu(\text{B-O})$ , 887  $\nu(\text{B-Ph})$ , 1367  $\nu(\text{N-O})$ , 744 and 701  $\nu(\text{Ar-H})$ . <sup>1</sup>H-NMR (CDCl<sub>3</sub>, TMS,  $\delta$  ppm)  $\delta$ : 7.39–7.28 (m, 20H, Ar-CH), 7.19–7.16 (m, 20H, Ar-CH), 5.29–5.27 (d, 4H, NH,  $J = 8$  Hz), 3.51 (s, 8H, N-<sup>5</sup>CH<sub>2</sub>), 2.91–2.88 (d, 4H, N-CH,  $J = 12$ ), 2.08–2.04 (d, 16H, N-<sup>6</sup>CH<sub>2</sub>,  $J = 16$ ), 1.92–1.88 (m, 8H, C-<sup>7</sup>CH<sub>2</sub>) and 1.66–1.61 (m, 8H, C-<sup>7</sup>CH<sub>2</sub>). <sup>13</sup>C-NMR (CDCl<sub>3</sub>, TMS,  $\delta$  ppm): C<sub>1</sub> (127.11), C<sub>2</sub> (128.38), C<sub>3</sub> (128.78), C<sub>4</sub> (137.74), C<sub>5</sub> (62.79), C<sub>6</sub> (53.03), C<sub>7</sub> (34.01), C<sub>8</sub> (52.09) C<sub>9</sub> (148.57), C<sub>10</sub> (131.98), C<sub>11</sub> (127.33), C<sub>12</sub> (127.19) and C<sub>13</sub> (126.05).

### 2.4 Synthesis of the metal complexes [Ni(L)<sub>2</sub>Cu<sub>2</sub>(X)<sub>2</sub>](ClO<sub>4</sub>)<sub>2</sub>

The mononuclear nickel complex (1) (0.4 g, 0.51 mmol) was added to Et<sub>3</sub>N (0.25 mmol) in abso-

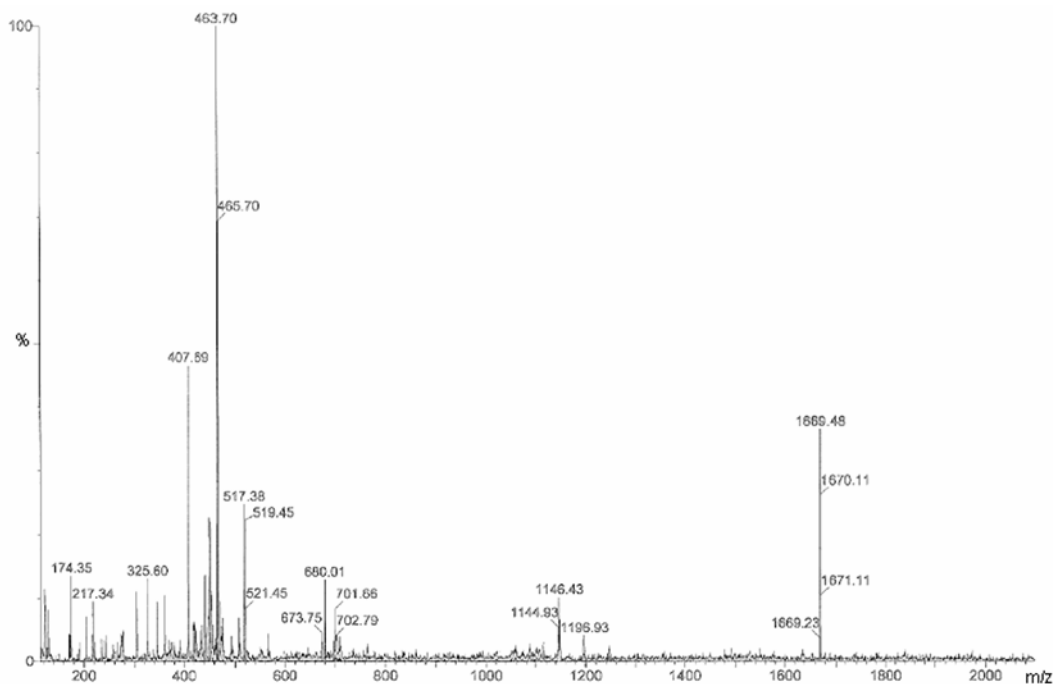


**Figure 1.** The mass spectrum of metal complex (3).

**Table 1.** The formula, formula weight, colours, melting points, molar conductivity, yields, magnetic susceptibilities and elemental analyses results of the compounds.

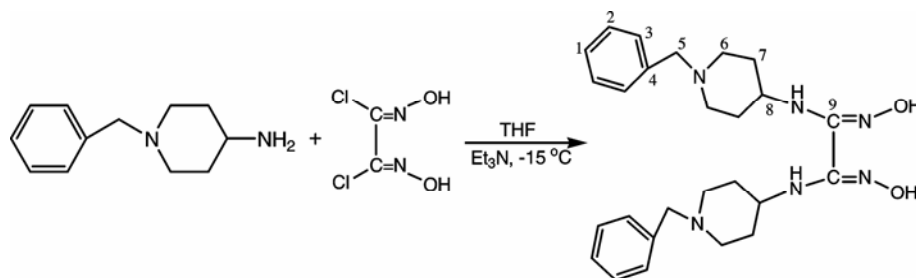
Compounds	FW (g/mol)	Colour	dec.point (°C)	$\Lambda_M$ ( $\Omega^{-1}\text{cm}^2$ $\text{mol}^{-1}$ )	Yield (%)	$\mu_{\text{eff}}$ [BM]	Elemental analyses % calculated (found)		
							C	H	N
Ligand (LH <sub>2</sub> ) C <sub>26</sub> H <sub>35</sub> N <sub>6</sub> O <sub>2</sub>	465	Yellow	142–145	–	84	–	67.24 (67.21)	7.76 (7.62)	18.10 (17.98)
Complex (1) C <sub>52</sub> H <sub>70</sub> N <sub>12</sub> O <sub>4</sub> Ni	985	Red	215–220	36.5	62	Dia	63.35 (63.23)	7.10 (7.16)	17.05 (17.09)
Complex (2) C <sub>76</sub> H <sub>88</sub> N <sub>12</sub> O <sub>4</sub> B <sub>2</sub> Ni	1313	Orange	118–122	18.7	58	Dia	69.46 (69.31)	6.70 (6.76)	12.80 (12.89)
Complex (3) C <sub>76</sub> H <sub>84</sub> N <sub>16</sub> O <sub>12</sub> Cl <sub>2</sub> NiCu <sub>2</sub>	1669	Dark green	170–173	162	56	1.38	54.64 (54.38)	5.03 (5.08)	13.42 (13.34)
Complex (4) C <sub>72</sub> H <sub>84</sub> N <sub>16</sub> O <sub>12</sub> Cl <sub>2</sub> NiCu <sub>2</sub>	1639	Dark green	225–230	165	50	1.32	52.72 (52.58)	5.28 (5.16)	13.66 (13.71)
Complex (5) C <sub>72</sub> H <sub>92</sub> N <sub>16</sub> O <sub>16</sub> Cl <sub>2</sub> NiCu <sub>2</sub>	1685	Dark green	218–221	183	58	1.26	51.27 (51.28)	5.46 (5.53)	13.29 (13.55)

\*bpy = bipyridine, phen = 1,10-phenanthroline

lute ethanol (60 ml) and the mixture was stirred for 1.5 h. The separated solution of Cu(ClO<sub>4</sub>)<sub>2</sub>·6H<sub>2</sub>O (0.38 g, 1.0 mmol) for [Ni(L)<sub>2</sub>Cu<sub>2</sub>(1,10-phen)<sub>2</sub>] (3), [Ni(L)<sub>2</sub>Cu<sub>2</sub>(2,2'-bpy)<sub>2</sub>] (4) and [Ni(L)<sub>2</sub>Cu<sub>2</sub>(4,4'-bpy)<sub>2</sub>(H<sub>2</sub>O)<sub>2</sub>] (5) in absolute ethanol (15 ml) and 1,10-phenanthroline monohydrate (0.2 g, 1.0 mmol), 2,2'-bipyridine (0.16 g, 1.0 mmol) or 4,4'-bipyridine (0.16 g, 1.0 mmol) in absolute ethanol (15 ml) was

successively added to the resulting mixture, which was boiled under reflux for 6–7 h. The dark green product was filtered, washed with EtOH, MeOH and Et<sub>2</sub>O. Then dried *in vacuo* at 35°C.

2.4a [Ni(L)<sub>2</sub>Cu<sub>2</sub>(1,10-phen)<sub>2</sub>](ClO<sub>4</sub>)<sub>2</sub> (3): IR (KBr pellets,  $\nu_{\text{max}}/\text{cm}^{-1}$ ): 3386  $\nu$ (NH), 3060–3019  $\nu$ (Ar-H), 2954–2758  $\nu$ (Aliph-H), 1600  $\nu$ (C=N), 1367

Scheme 1. Synthesis of ligand (LH<sub>2</sub>).

$\nu(\text{N-O})$ , 1098 and 624  $\nu(\text{ClO}_4)$ . MS (LSI, Scan ES<sup>+</sup>):  $m/z$  (%) 1669.5 and (36) [M]<sup>+</sup>, 1146.4 (10), 680.0 (10), 517.4 (25), 463.7 (100), 407.7 (45) and 174.4 (15) (figure 5).

2.4b  $[\text{Ni}(\text{L})_2\text{Cu}_2(2,2'\text{-bpy})_2](\text{ClO}_4)_2$  (**4**): 3659–3143  $\nu(\text{H}_2\text{O}/\text{NH})$ , 3061–3025  $\nu(\text{Ar-H})$ , 2938–2764  $\nu(\text{Aliph-H})$ , 1600  $\nu(\text{C=N})$ , 1364  $\nu(\text{N-O})$ , 1091 and 626  $\nu(\text{ClO}_4)$ . MS (LSI, Scan ES<sup>+</sup>):  $m/z$  (%) 1640.4 (13) [M + 1]<sup>+</sup>, 1146.3 (10), 469.4 (100), 313.2 (22), 242.3 (45) and 174.3 (15).

2.4c  $[\text{Ni}(\text{L})_2\text{Cu}_2(4,4'\text{-bpy})_2(\text{H}_2\text{O})_2](\text{ClO}_4)_2$  (**5**): 3629–3114  $\nu(\text{H}_2\text{O}/\text{NH})$ , 3061–3031  $\nu(\text{Ar-H})$ , 2924–2759  $\nu(\text{Aliph-H})$ , 1602  $\nu(\text{C=N})$ , 1361  $\nu(\text{N-O})$ , 1090 and 626  $\nu(\text{ClO}_4)$ .

### 3. Results and discussion

The synthetic route for the ligand (LH<sub>2</sub>) is given in scheme 1. The analytical data of (**1**) metal complex indicates 1 : 2 metal/ligand stoichiometry. The analytical data of (**2**) and  $[\text{Ni}(\text{LH})_2\text{Cu}_2(\text{X})_2](\text{ClO}_4)_2$  (**3**), (**4**), (**5**) (where X = 1,10-phenanthroline, 2,2'-bipyridine, and 4,4'-bipyridine) metal complexes indicate 3 : 2 : 2 metal/ligand/other groups. BPh<sub>2</sub><sup>+</sup> cation formed BPh<sub>4</sub><sup>-</sup> anion. May be we expected oligomerization of complex (**5**) since one nitrogen of the 4,4'-bipyridyl moiety is suggested coordinated to Cu(II) and other one free. We have attempted to prepare single crystals of ligand (LH<sub>2</sub>) and metal complexes (**1**), (**2**), (**3**), (**4**) and (**5**) in different solvents, but we could not prepare convenient single crystals of ligand and metal complexes. Also, the spectroscopic results shown that these compounds are of high probability as proposed structures.

The fragments observed in the mass spectrum of the complexes are useful for characterization of the metal complexes. The mass spectra of metal complexes (**3**) and (**4**) show molecular ion peaks [M]<sup>+</sup> at

1669.5 and 1640.4 (figure 1) respectively, which confirm the proposed structures of the metal complexes (**3**) and (**4**). It is a proof for such a hypotheses came from the ESI-MS spectra of compounds. As shown in figure 1, the presence of only two peak at  $m/z$  1669.2 and 1669.5 suggested that  $[\text{Ni}(\text{L})_2\text{Cu}_2(1,10\text{-phen})_2](\text{ClO}_4)_2$  species should be the main species, indicating that in the presence of Ni and Cu ion.<sup>19</sup> The structures presented in this paper are proposed based on the mass analysis.

#### 3.1 NMR results

The data of the <sup>1</sup>H and <sup>13</sup>C-NMR spectra obtained for ligand (LH<sub>2</sub>), metal complexes (**1**) and (**2**) in CHCl<sub>3</sub>-d<sub>1</sub> are given in the experimental section. The chemical shifts were observed at 9.56 ppm as singlet for =N-OH groups of oximes in the <sup>1</sup>H NMR spectra of ligand (LH<sub>2</sub>). The chemical shifts which belong to -NH protons were observed at 5.15–5.13 ppm as a doublet for LH<sub>2</sub>, at 4.80–4.77 ppm as a doublet for complex (**1**) (figure 2) and at 5.29–5.27 ppm as a doublet for complex (**2**), respectively and disappeared with D<sub>2</sub>O exchange. The <sup>1</sup>H-NMR resonans with expected integrated intensities were observed 7.31–7.26 ppm corresponding to the Ar-CH, 3.50 ppm corresponding to the N-<sup>5</sup>CH<sub>2</sub>, 2.82–2.80 ppm corresponding to the N-CH, 2.07–2.01 ppm corresponding to the N-<sup>6</sup>CH<sub>2</sub>, 1.85–1.83 and 1.60–1.55 ppm corresponding to the C-<sup>7</sup>CH<sub>2</sub>, respectively. The <sup>1</sup>H-NMR spectra of the diamagnetic metal complex (**1**) was characterized by the existence of intra-molecular D<sub>2</sub>O-exchangeable H-bridge (O-H...O) protons which were observed by a new signals at low field,  $\delta = 16.49$  ppm for complex (**1**). The other protons were observed at different field than ligand. In the <sup>1</sup>H-NMR spectra of complex (**1**), the D<sub>2</sub>O-exchangeable hydrogen-bridged protons, which were evident in complex (**1**), disappear after the formation of the BPh<sub>2</sub><sup>+</sup>-bridged complex.

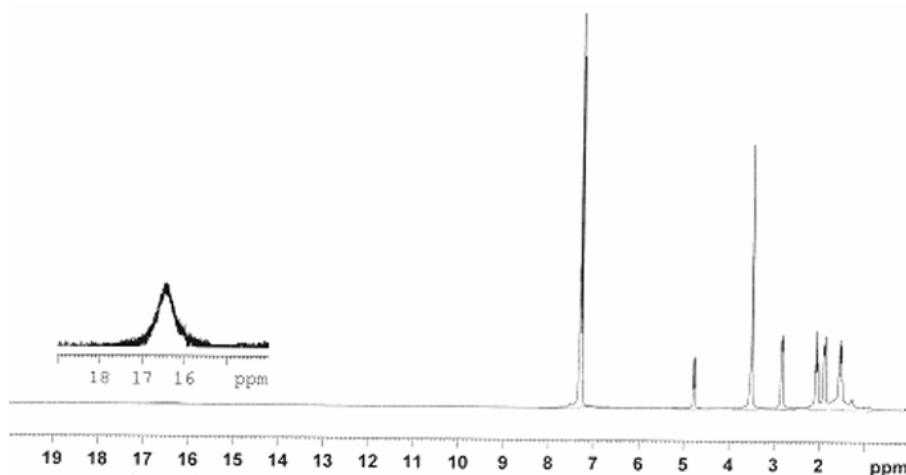


**Figure 2.** The  $^1\text{H}$ -NMR spectrum of metal complex (1).

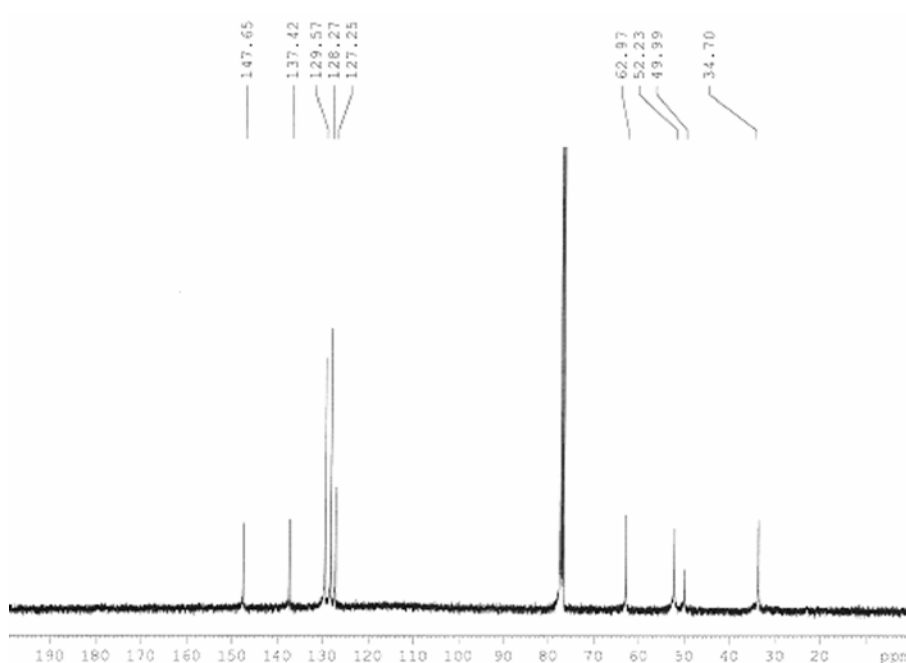


**Figure 3.** The  $^{13}\text{C}$ -NMR spectrum of the ligand ( $\text{LH}_2$ ).

Indeed, the chemical shifts of the aromatic protons are obtained at 7.33–7.28 ppm as multiplets for complex (1), whereas the chemical shifts of the aromatic protons are obtained at 7.39–7.28 and 7.19–7.16 ppm as multiplets for complex (2), which proves that the (O–H $\cdots$ O) bridges between the molecules are replaced by  $\text{BPh}_2^+$  cation formed  $\text{BPh}_4^-$  anion.<sup>20</sup> More detailed information about the structure of  $\text{LH}_2$  is provided by the  $^{13}\text{C}$ -NMR spectrum (figure 3). The chemical shifts for the amide carbon atoms are found at 147.65 ppm.<sup>20,21</sup> These equivalent

carbon atoms, especially belonging to, hydroxy-imino carbon atoms, also confirm the *anti* structure of  $\text{LH}_2$ .<sup>22</sup> The chemical shifts of the aromatic carbon atoms are obtained at 138.31, 129.00, 128.25 and 127.08 ppm for complex (1), whereas the chemical shifts of the aromatic carbons are obtained 137.74, 131.98, 128.78, 128.38, 127.33, 127.19, 127.11 and 126.05 ppm for complex (2), which proves that the (O–H $\cdots$ O) bridges between the molecules are replaced by  $\text{BPh}_2^+$  (figure 4). The other chemical shifts ( $^1\text{H}$  and  $^{13}\text{C}$ -NMR) belong to  $\text{BPh}_2^+$ -capped  $\text{Ni}^{\text{II}}$  metal

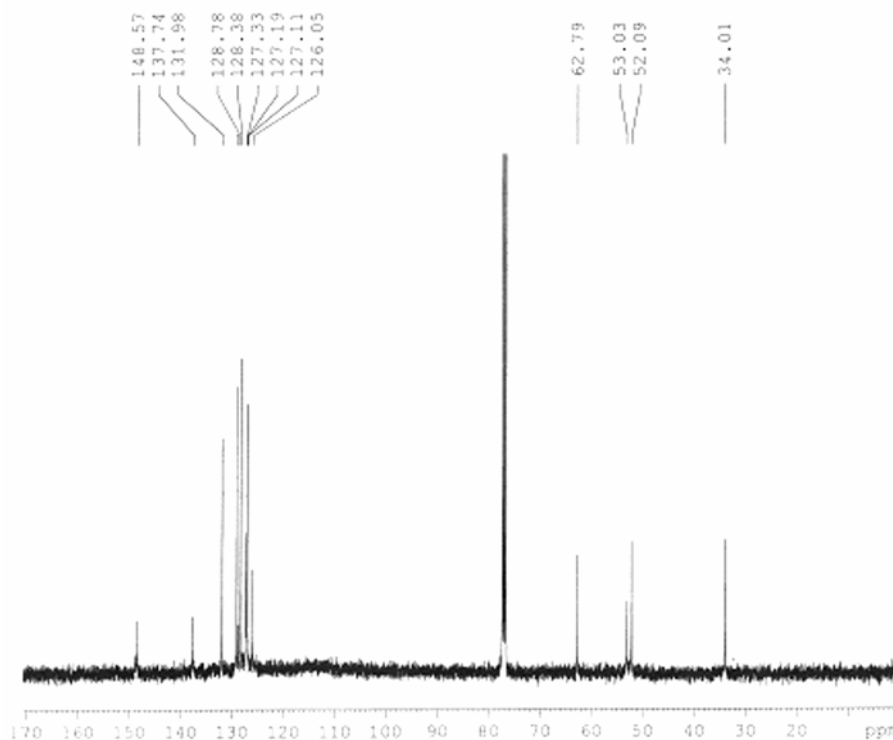


**Figure 4.** The  $^{13}\text{C}$ -NMR spectrum of the metal complex (2).

complex (2) are very similar to those for the H-bonded  $\text{Ni}^{\text{II}}$  metal complex (1).

### 3.2 IR results

The infrared spectra of ligand ( $\text{LH}_2$ ) with its mononuclear metal complex (1) and (2) with trinuclear metal complexes (3), (4) and (5) have been studied in order to characterize their structures (figure 5). The IR spectra of the free ligand and its metal chelates were carried out in the  $4000\text{--}400\text{ cm}^{-1}$  range. The IR spectra of all metal complexes were interpreted by comparing the spectra with those of the free ligand. The characteristic infrared spectrum data are given in experimental section. In the IR spectrum of ligand, the  $\nu(\text{O-H/N-H})$  stretching vibrations were observed between  $3617$  and  $3143\text{ cm}^{-1}$  for  $\text{LH}_2$ . The free *vic*-dioxime ligand showed a strong peak at  $1638\text{ cm}^{-1}$  for  $\text{LH}_2$ , which is characteristic of the azomethine  $\nu(\text{C=N})$  group.<sup>23</sup> The  $\nu(\text{C=N})$  stretching vibrations are affected upon complexation and are situated at a frequency significantly different than the free ligands. Coordination of the *vic*-dioxime ligands to the metal center through the four nitrogen atom are expected to reduce the electron density in the azomethine link and

lower the  $\nu(\text{C=N})$  absorption frequency. The peak due to  $\nu(\text{C=N})$  are shifted to lower frequencies and appears between  $1616\text{--}1599\text{ cm}^{-1}$ , indicating coordination of the azomethine nitrogen to the nickel metal.<sup>24</sup> However, the disappearance of  $\nu(\text{O-H})$  stretching bands in the IR spectrum of free ligand together with the existence of H-bridge ( $\text{O-H}\cdots\text{O}$ ) at  $1726\text{ cm}^{-1}$  and the shifting of  $-\text{C=N}$  and  $-\text{N-O}$  stretches in the IR spectra of the metal complex (1) provide support for  $\text{MN}_4$ -type coordinations in the metal complexes.<sup>25</sup> The IR spectrum of  $\text{BPh}_2^+$ -bridged  $\text{Ni}^{\text{II}}$  complex (2) is similar to the H-bridged  $\text{Ni}^{\text{II}}$  complex (1). The stretching vibration of ( $\text{O-H}\cdots\text{O}$ ) bond at  $1726\text{ cm}^{-1}$  disappeared upon encapsulation of the H-bonded complex with the appearance of peaks due to the  $\text{BPh}_2^+$  contaminant around  $1195$  and  $887\text{ cm}^{-1}$  for B-O and B-Ph groups, respectively.<sup>20</sup> In the IR spectra of trinuclear metal complexes (3), (4) and (5), the intramolecular hydrogen band was not observed, as expected. This is because the H-bonded ( $\text{O-H}\cdots\text{O}$ ) of mononuclear nickel complex disappeared on an encapsulation of the copper ions on the formation of trinuclear metal complexes, namely  $\text{Cu}_2(1,10\text{-phen})_2$ ,  $\text{Cu}_2(2,2'\text{-bpy})_2$  or  $\text{Cu}_2(4,4'\text{-bpy})_2$ . Perchlorate salts show strong antisymmetric stretching band between  $1098$  and  $1090\text{ cm}^{-1}$  and

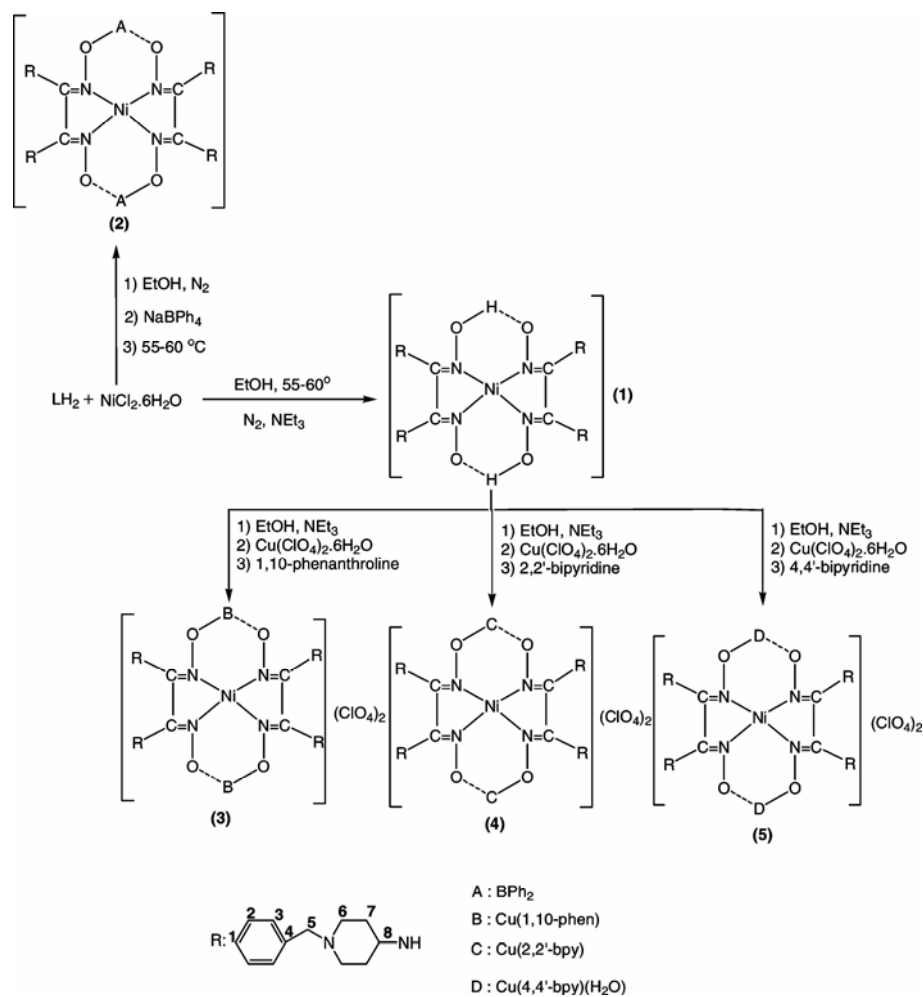


**Figure 5.** The proposed structure for the metal complexes.

sharp antisymmetric stretching band between 626 and 624  $cm^{-1}$ , an indication of uncoordinated perchlorate anions.<sup>26,27</sup>

### 3.3 UV-Vis spectra

Electronic spectra of ligand ( $LH_2$ ) and their mononuclear metal complexes (1) and (2), trinuclear, metal complexes (3), (4) and (5) have been recorded in the 200–1100 nm range in  $CHCl_3$  and DMF solutions and their corresponding data are given in table 2. Each ligand and mono with trinuclear metal complexes show several absorptions in the visible and ultraviolet region. The UV-Vis spectra of the ligand and metal complexes in  $CHCl_3$  showed two to six numbers of absorption bands between 230 and 795 nm and in DMF showed two to seven numbers of absorption bands between 268 and 734 nm, respectively. The wavelengths of absorption bands

appeared in the UV region in both solvents are practically identical. The bands below 455 nm in  $C_2H_5OH$  or  $CHCl_3$  are almost certainly associated with intraligand  $\pi \rightarrow \pi^*$  and  $n \rightarrow \pi^*$  or charge-transfer transitions.<sup>28</sup> In the electronic spectra of the ligand and their metal complexes, the wide range bands seems to be due to both the  $\pi \rightarrow \pi^*$ ,  $n \rightarrow \pi^*$  and  $d-d$  transitions of (C=N) and charge-transfer transition arising from  $\pi$  electron interactions between the metal and ligand which involves either a metal-to-ligand or ligand-to-metal electron transfer.<sup>29,30</sup> The absorption bands below 295 nm in  $CHCl_3$  or DMF are practically identical and can be attributed to  $\pi \rightarrow \pi^*$  transitions in the benzene ring or azomethine (C=N) groups. The absorption bands observed within the range of 332–368 nm in  $CHCl_3$  and the range of 331–397 nm in DMF are most probably due to the transition of  $n \rightarrow \pi^*$  of imine group corresponding to the ligand or metal com-

**Table 2.** Characteristic UV-Vis bands of the ligand and metal complexes.

Compounds	Solvents	Wave length ( $\lambda_{\max}$ (nm) (log $\epsilon$ ))					
(LH <sub>2</sub> )	CHCl <sub>3</sub>	230 (5.52)	242 (4.79)				
	DMF	268 (4.82)	353* (4.52)				
(1)	CHCl <sub>3</sub>	248 (4.07)	260 (4.24)	332 (3.74)	364 (3.21)	451* (2.86)	565* (2.03)
	DMF	269 (5.16)	364 (5.11)	443 (4.64)			
(2)	CHCl <sub>3</sub>	242 (5.27)	292* (4.79)	352 (4.31)	368 (4.36)	449 (3.82)	563* (2.17)
	DMF	272 (4.98)	363 (4.65)	402 (3.86)			
(3)	CHCl <sub>3</sub>	242 (4.35)	270 (4.14)	345* (3.84)	428* (3.54)	560 (2.76)	
	DMF	275 (5.28)	342 (4.73)	424 (4.28)	569 (3.76)	727 (2.59)	
(4)	CHCl <sub>3</sub>	240 (5.62)	257 (5.53)	279 (4.61)	295* (4.34)	366 (4.04)	453* (3.60)
	DMF	278 (5.44)	286 (5.04)	304 (4.82)	350 (4.56)	427 (3.94)	569 (3.21) 734 (2.95)
(5)	CHCl <sub>3</sub>	240 (5.32)	273* (5.05)	338 (4.86)	455 (3.92)	580 (3.06)	795 (2.74)
	DMF	271 (5.26)	331 (5.07)	397 (4.84)	618 (3.81)		

\* = Shoulder peak, \*\* bpy = bipyridine, phen = 1,10-phenanthroline

plexes.<sup>31</sup> The weak  $d-d$  transitions for mononuclear complex (1) and (2), could be observed between 443 and 565 nm and trinuclear metal complexes (3), (4) and (5) could be observed between 424 and 795 nm in CHCl<sub>3</sub> or DMF, respectively. These absorption bands are typical for nickel(II) complexes with a square-planar structure.<sup>31,32</sup>

### 3.4 Magnetic moments and molar conductivity

Magnetic susceptibility measurements provide sufficient data to characterize the structure of the metal complexes. Magnetic moments measurements of all metal complexes carried out at 25°C. The results show that mononuclear metal complexes (1) and (2) are diamagnetic, indicating the low-spin ( $S = 0$ ) square planar  $d^8$ -systems, whereas magnetic moments of the trinuclear metal complexes (3), (4) and (5) are found between 1.38 and 1.26 B.M. for per Cu(II) molecule. It is obvious that the metal complexes possess antiferromagnetic properties at room temperature by strong intramolecular antiferromagnetic spin exchange interaction as reported previously for trinuclear copper complexes with oximate bridge ligands.<sup>27,33</sup> Since the metal complexes (1) and (2) are diamagnetic, their NMR spectra could be obtained. The absorption bands observed for the electronic spectra of (1) and (2) metal complexes also support the square-planar geometry<sup>34</sup> (table 2).

The ligand (LH<sub>2</sub>) are soluble in common organic solvents such as THF, C<sub>2</sub>H<sub>5</sub>OH, CH<sub>2</sub>Cl<sub>2</sub>, and DMSO. Although mononuclear metal complex (1) is soluble in DMSO and DMF and slightly soluble in CH<sub>2</sub>Cl<sub>2</sub>, CHCl<sub>3</sub>, mononuclear metal complex (2) and

trinuclear metal complexes (3), (4) and (5) are highly soluble in DMSO, DMF CH<sub>2</sub>Cl<sub>2</sub>, CHCl<sub>3</sub> and (CH<sub>3</sub>)<sub>2</sub>CO due to the presence of BPh<sub>2</sub><sup>+</sup> cation formed BPh<sub>4</sub><sup>-</sup> anion, Cu<sub>2</sub> (1,10-phen)<sub>2</sub>, Cu<sub>2</sub> (2,2'-bpy)<sub>2</sub> or Cu<sub>2</sub> (4,4'-bpy)<sub>2</sub> bridged groups in the oxime moieties. All complexes are stable in the solvents reported in this study at room temperature. With a view to studying the electrolytic nature of the metal complexes, their molar conductivities were measured in DMF (N,N-dimethyl formamide) at 10<sup>-3</sup> M. The molar conductivity ( $\Lambda_M$ ) values of metal complexes (1) and (2) are in the range of 36.5–18.7  $\Omega^{-1}$  cm<sup>2</sup> mol<sup>-1</sup> at room temperature,<sup>35</sup> indicating their almost non-electrolytic nature. Due to non-free ions in metal complexes (1) and (2), the results indicate that these metal complexes are poor in molar conductivity. The molar conductivities ( $\Lambda_M$ ) values of these trinuclear metal complexes (3), (4) and (5) are in the range of 162–183  $\Omega^{-1}$  cm<sup>2</sup> mol<sup>-1</sup> at room temperature, indicating 1:2 electrolytes or three ionic species in solution.<sup>31b</sup>

### 3.5 Crystallography

We have attempted to prepare single crystals of ligand (LH<sub>2</sub>) and metal complexes (1), (2), (3), (4) and (5) in different solvents, but we could not prepare convenient single crystals of ligand and metal complexes. However, the crystalline nature of metal complexes (1), (2), (3), (4) and (5) can be readily evidenced from their X-ray powder patterns. Metal complexes (1), (2), (3), (4) and (5) exhibit sharp reflections and all diffractograms are nearly identical, indicating the isostructural nature of the four compounds. Also, the large number of reflections as well

**Table 3.** Voltammetric data for the complexes in DMSO–TBAP.

Complexes	L/L <sup>a</sup> $E_{1/2}$ (V)	Ni(II)/Ni(I) <sup>b</sup> $E_{pc}$ (V)	Cu(I)/Cu(0) $E_{pc}$ (V)	Cu(II)/Cu(I) $E_{pc}$ (V)	Ni(II)/Ni(III) <sup>b</sup> $E_{pa}$ (V)	Cu(II)/Cu(III) $E_{pa}$ (V)	L/L <sup>+</sup> $E_{pa}$ (V)
(1)	1.51 (0.10) <sup>c</sup>	-1.12			0.59		0.70
(2)		-1.50			0.35 <sup>a</sup> (0.11) <sup>c</sup>		
(3)		-1.16	-0.61	-0.17		0.85	
(4)		-1.07	-0.53	-0.01		0.85	
(5)		-1.14	-0.56	-0.05		0.83	

$${}^a E_{1/2} = E_{pc} + E_{pa}/2$$

<sup>b</sup>Cathodic peak potential for reduction, anodic peak potential for oxidation for irreversible processes

$${}^c \Delta E_p = E_{pc} - E_{pa} \text{ at } 0.100 \text{ V s}^{-1} \text{ scan rate}$$

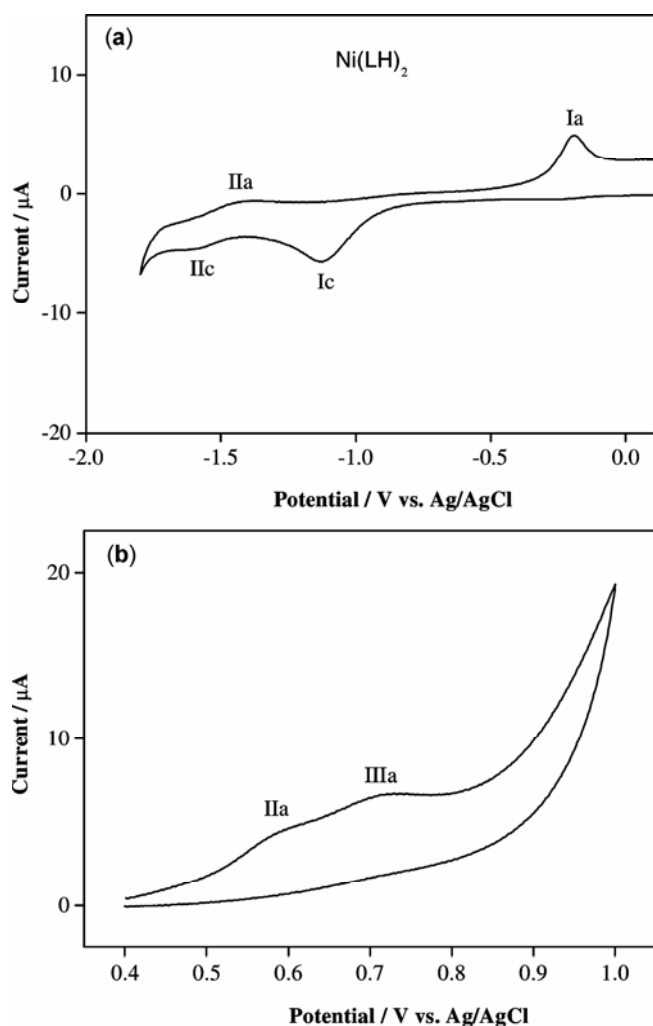


**Figure 6.** Cyclic voltammograms of metal complex (1) in DMSO solution containing 0.1 M TBAP. (a) cathodic sweep and (b) anodic sweep, scan rates =  $0.100 \text{ V s}^{-1}$ .

as their positions indicate a low crystal symmetry.<sup>36</sup> This results show that metal complexes (1), (2), (3), (4) and (5) are indicating crystalline nature, not amorphous nature. Whereas, the X-ray powder pat-

tern of the ligand ( $\text{LH}_2$ ) exhibited only broad humps, indicating its amorphous nature.

### 3.6 Electrochemistry

The electrochemical properties of metal complexes (1), (2), (3), (4) and (5) were investigated using cyclic voltammetric techniques in DMSO containing 0.1 M TBAP. The data obtained in this work are listed in table 3. Figures 6a–b represent the cyclic voltammetry (CV) of complex (1) at  $0.100 \text{ V s}^{-1}$  scan rate. As seen from figure 6a, complex (1) displayed two reduction waves in DMSO containing Ag/AgCl electrode system. The cathodic peak potential of the first reduction process was observed at  $E_{pc} = -1.12 \text{ V}$  versus Ag/AgCl. The reduction process has the large value of the cathodic to the anodic peak separation ( $\Delta E = 0.93 \text{ V}$ ) at  $0.100 \text{ V s}^{-1}$  scan rate, which indicates an irreversible process of the first reduction process in the scan range of  $0.025$ – $0.250 \text{ V s}^{-1}$  in DMSO. No couple was recorded during cathodic sweep range  $0.10$ – $0.75 \text{ V}$ , indicating that the wave observed at  $E_{pa} = -0.19 \text{ V}$  corresponds to the first reduction process. The second reduction wave belongs to the ligand-based process. It is assigned to a reversible character with the convenient values of the cathodic to the anodic peak separation ( $\Delta E = 0.10 \text{ V}$  at  $0.100 \text{ V s}^{-1}$  scan rate). The reduction process refers to the metal-based  $\text{Ni}^{\text{II}}/\text{Ni}^{\text{I}}$  couples (Ic). The redox process of the metal centered in *vic*-dioxime complexes are mostly observed at more positive values than that of the ligand-based processes.<sup>28,35b,37–41</sup> It is also seen that the peak cathodic and peak anodic current ratios,  $i_{pc}/i_{pa}$  for the second reduction waves approaches almost unity, which indicates that this electrochemical reaction was not accompanied by any other physical or chemical processes throughout the electrochemical timescale.

The cathodic to the anodic peak separation ( $\Delta E$ ) observed for the second reduction process is a little larger than expected theoretically for a reversible one-electron process. However, under our experimental conditions, the peak separation of the ferrocene/ferrocenium couple was observed to be 70–120 mV in the scan rate of 0.025–0.500  $\text{Vs}^{-1}$ , which can be used as a criterion for electrochemical reversibility.<sup>42</sup> The peak separation increases only slightly with increasing scan rate, and the case is true for the ferrocene/ferrocenium couple under our experimental conditions. The half-wave potential of the second reduction process is  $E_{1/2} = -1.51$  V vs Ag/AgCl. Figure 6b indicates oxidation of complex (1), which displaces a anodic peak potential at  $E_{\text{pa}} = -0.59$  V (couple IIa) without corresponding anodic wave. This oxidation is a irreversible process

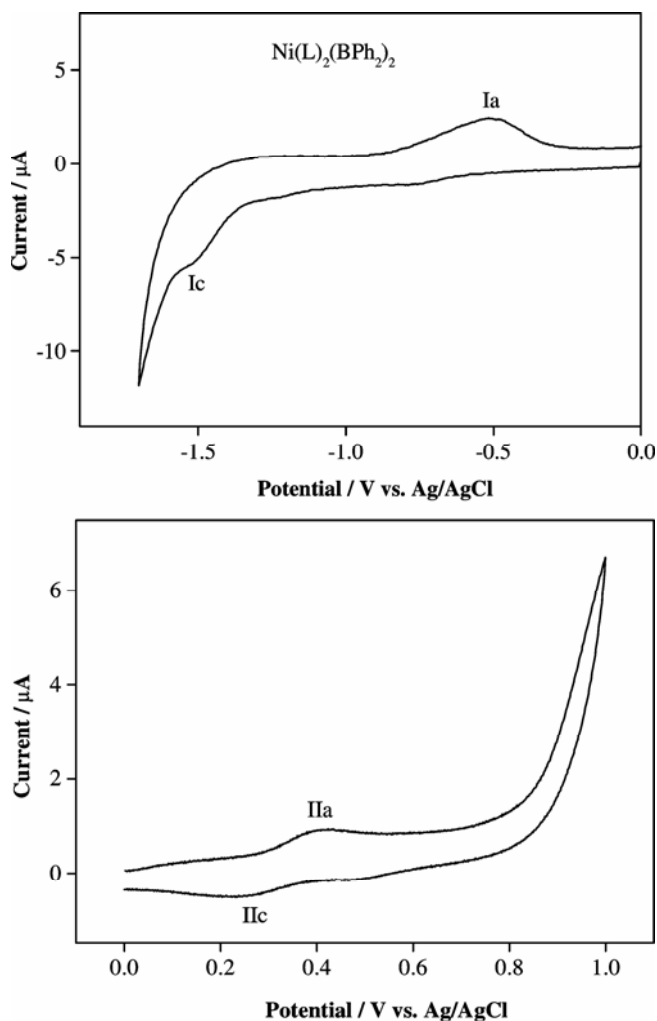


**Figure 7.** Cyclic voltammograms of metal complex (2) in DMSO solution containing 0.1 M TBAP. (a) cathodic sweep and (b) anodic sweep, scan rates = 0.100  $\text{V s}^{-1}$ .

and based on the metal center,  $\text{Ni}^{\text{II}}/\text{Ni}^{\text{III}}$  couples. The couple (IIIa) observed at a more positive potential probably belongs to the ligand-based process. Figures 7a–b indicate the redox processes of complex (2) during cathodic and anodic sweep at the scan rate of 0.010  $\text{Vs}^{-1}$  in DMSO. As seen from figure 7a, complex (2) exhibits one reduction process based on the metal, which is referred to  $\text{Ni}^{\text{II}}/\text{Ni}^{\text{I}}$  couples (Ic). This process almost exhibits a similar behaviour what is observed for complex (1) in the same experimental conditions. However, its cathodic peak potential was observed at  $E_{\text{pc}} = -1.50$  V, which shifted toward more negative value compared to that of complex (1), probably due to decreasing effect of back donation of metal-oxime moieties as a result of the  $\text{BPh}_2^+$ -bridged complex formation. The similar effect was also observed in the peak potential of the reoxidation wave (Ia). No reduction process based on the ligand was observed during the cathodic sweep in the potential range 0.00–1.80 V (vs Ag/AgCl) in DMSO. It was probably shifted to out of potential range. The complex (2) exhibits one electron oxidation process based on the  $\text{Ni}^{\text{II}}/\text{Ni}^{\text{III}}$  couples (figure 7b). The oxidation wave shows the convenient values of the cathodic to the anodic peak separation ( $\Delta E = 0.11$  V at 0.10  $\text{V s}^{-1}$  scan rate). Also, the peak cathodic and peak anodic current ratios,  $i_{\text{pc}}/i_{\text{pa}}$  for the oxidation waves approached almost unity. Both of which are assigned to the reversible character for mono-oxidized species in DMSO solution. The half-peak potential of the process is  $E_{1/2} = 0.35$  V versus Ag/AgCl at

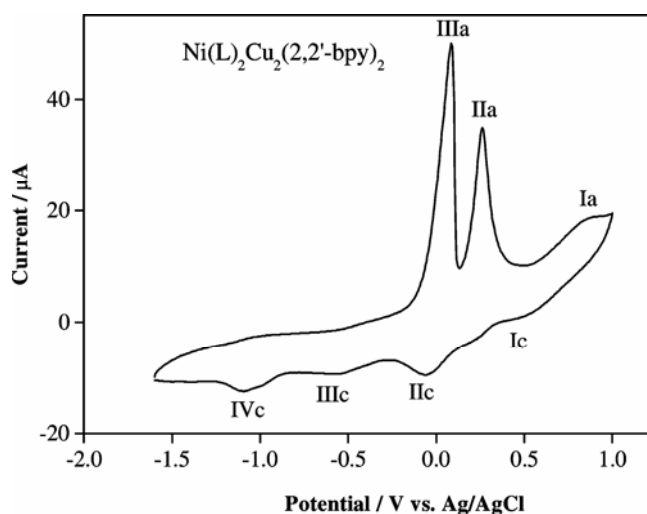


**Figure 8.** Cyclic voltammograms of metal complex (4) in DMSO solution containing 0.1 M TBAP. Scan rates = 0.100  $\text{V s}^{-1}$ .

0.010  $\text{Vs}^{-1}$  scan rate. It can be concluded from the result that the  $\text{BPh}_2^+$ -bridged complex formation increases the stability of the mono-oxidized species compared to complex (1) in the same experimental conditions. The CV of the trinuclear copper complexes (3), (4) and (5), showed considerably different behaviour compared with those of the metal complexes (1) and (2) in the same experimental conditions because of the copper metals centered at the bridge formation. All copper complexes showed almost similar electrochemical fashion in DMSO. An example of the CVs of the complexes is presented in figure 8 where metal complex (4) indicates three reduction waves at potential range 0.0–1.6 V. The cathodic peak potentials of the complex were appeared at  $E_{\text{pc}} = 0.01, -0.53$  and  $-1.07$  V, which were assigned to the copper-based reduction processes, namely  $\text{Cu}^{\text{II}}/\text{Cu}^{\text{I}}$  (IIc),  $\text{Cu}^{\text{I}}/\text{Cu}^0$  (IIIc), and nickel-based reduction process,  $\text{Ni}^{\text{II}}/\text{Ni}^{\text{I}}$  (IVc), respectively. The copper-based reduction waves (IIc and IIIc) have corresponding anodic waves (IIa and IIIa) while nickel-based reduction process has no corresponding anodic wave. The complex also exhibited one oxidation process at  $E_{\text{pc}} = 0.85$  V (Ia). The oxidation wave (Ia) has corresponding cathodic wave (Ic), which is probably attributable to  $\text{Cu}^{\text{II}}/\text{Cu}^{\text{III}}$  couples. Figure 9 shows the CV of complex (3) during cathodic sweep in the scan rate 0.01–0.10 V, where the inset figure indicates the plot of the anodic peak current versus scan rate. It was seen that direct proportionality of the anodic peak current

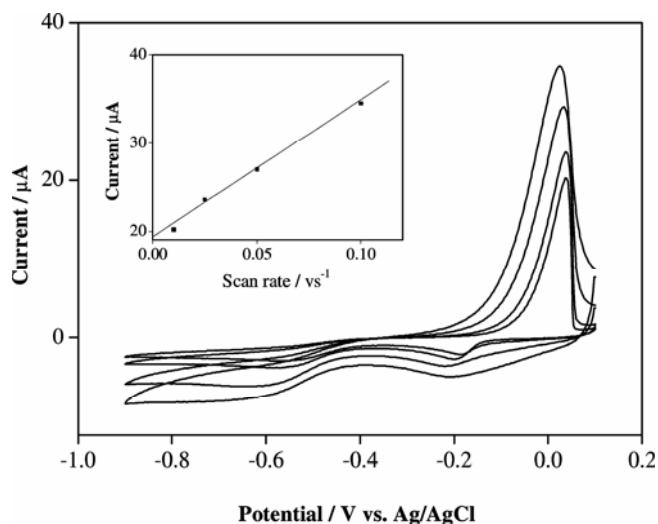


**Figure 9.** Cyclic voltammograms of metal complex (3) in DMSO solution containing 0.1 M TBAP in the potential range 0.10–0.90 V. Scan rates = 0.100  $\text{Vs}^{-1}$ . The inset figure shows the plot of current vs scan rate.

(IIIa) with the scan rate provided an evidence for the adsorption character of  $\text{Cu}^0/\text{Cu}^{\text{I}}$  wave.<sup>35,38–39,42</sup> The adsorption behaviour is also clearly seen from the high peak current ratio of reduced and reoxidized species corresponding to the copper center in the complex. All processes of the trinuclear complexes exhibited an irreversible fashion in the scan rate of 0.010–0.50  $\text{Vs}^{-1}$ . The corresponding data for the complexes are listed in table 3.

The spectroelectrochemical behaviour of metal complexes (1) and (2) were investigated using an *in situ* spectroelectrochemical technique including chronoamperometry and UV-Vis spectroscopy in DMSO solution containing 0.2 M TBAP. The UV-vis spectral changes for the reduced and oxidized species of the corresponding complexes were obtained in a thin-layer cell during applied potentials. The convenient applied potentials values for *in situ* spectroelectrochemical experiment were determined for each processes by taking CVs of the complexes in the thin-layer cell.

The complex (2) showed well-defined UV-Vis spectra during the first reduction processes ( $E_{\text{app}} = -1.65$  V) while the other complexes did not exhibit well-defined electronic spectra during the reduction or oxidation processes probably due their fast chemical decomposition or coupling during time scale of the spectroelectrochemical measurements. Figure 10 shows the UV-Vis spectral changes of complex (2), that is accompanied by the reduction process in the thin-layer cell. As can be seen, the spectra of the reduced species shows well-defined

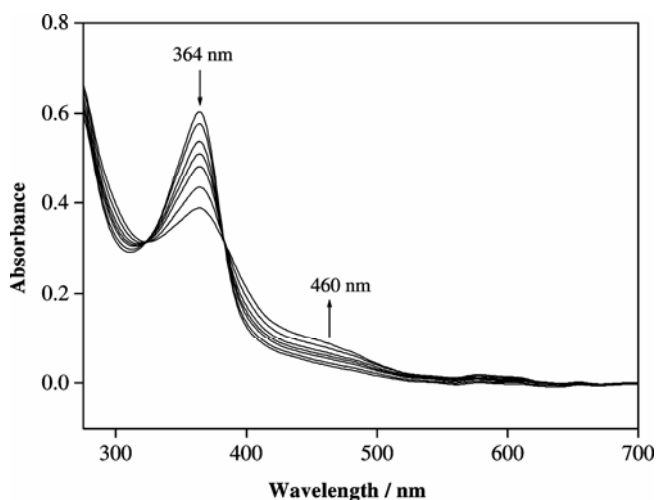


**Figure 10.** Time-resolved UV-Vis spectral changes of metal complex (2) during the reduction process at  $E_{\text{app}} = -1.65$  V in DMSO solution containing 0.2 M TBAP.

isosbestic points observed at  $\lambda = 323$  and  $383$  nm, confirming that the electrode reaction proceeds in a quantitative fashion and therefore the absence of any coupled chemistry.<sup>43–46</sup> The complex showed distinctive spectral changes that the intensity of the band ( $\lambda =$  at  $364$  nm, assigned to  $n \rightarrow \pi^*$  transitions) decreased and a new broad band in low intensity about  $460$  nm appeared as a result of the reduction of the nickel centered in the oxime core.

#### 4. Conclusions

In this study, the novel *vic*-dioxime ligand containing the 4-amino-1-benzyl piperidine group, *N,N'*-(4-amino-1-benzyl piperidine)-glyoxime, (LH<sub>2</sub>) and their mononuclear metal complexes (1) and (2) with trinuclear metal complexes (3), (4) and (5) were synthesized and characterized by elemental analyses, FT-IR, UV-Vis, <sup>1</sup>H and <sup>13</sup>C-NMR spectra, magnetic susceptibility measurements, molar conductivity, cyclic voltammetry, mass spectra and X-ray powder techniques. Although *vic*-dioximes complexes have been synthesized for a very long period of time, a few examples of their heteropolynuclear complexes have been studied. The most oxime metal complexes are slightly soluble in common organic solvents, which limit their practical usages for many purposes. This study presents highly soluble series of the mono- and trinuclear *vic*-dioxime complexes (2), (3), (4) and (5) which were prepared by the coordination of BPh<sub>2</sub><sup>+</sup>, Cu<sub>2</sub>(1,10-phen)<sub>2</sub>, Cu<sub>2</sub>(2,2'-bpy)<sub>2</sub> or Cu<sub>2</sub>(4,4'-bpy)<sub>2</sub> bridged groups into the main nickel oxime moieties. It is well known that the biological activities of mononuclear (1) and (2) with trinuclear metal complexes (3), (4) and (5) can be improved with mixed-ligand complexes with heterocyclic bases, such as 1,10-phenanthroline, 2,2'-bipyridine, 4,4'-bipyridine, pyridine, and BPh<sub>2</sub><sup>+</sup>. Therefore, the mononuclear (2) and the trinuclear metal complexes (3), (4) and (5) studied in the present work will be interesting for many applications in a variety of high technology fields, such as medicine, catalysis, as well as DNA binding and antitumor activity. The comparative electrochemical studies of mono and trinuclear complexes provide useful information on the electron-transfer reactions of the electro-reduced or electro-oxidized species in non-aqueous solution. Additionally, the results of the X-ray powder show that all metal complexes are indicating crystalline nature, not amorphous nature. Whereas, the ligand (LH<sub>2</sub>) exhibits only broad humps, indicating its amorphous nature.

#### Acknowledgements

This work has been supported (in part) by the Research Fund of Harran University (Sanliurfa, Turkey). This work has also been supported, in part, by the Turkish Academy of Sciences in the framework of the Young Scientist Award Program (TÜBA-GEBİP/2001).

#### References

- (a) Kurtoglu M, Dagdelen M M and Toroglu S 2006 *Trans. Met. Chem.* **31** 382; (b) Lauffer R B 1987 *Chem. Rev.* **87** 190; (c) Muise G T, Li X and Powell D R 2004 *Inorg. Chim. Acta* **357** 1134
- Chakravorty A 1974 *Coord. Chem. Rev.* **13** 1
- Leonardo J P, Novotnik D P and Neirinckx R D 1986 *J. Nucl. Med.* **27** 1819
- Dilworth J R and Parrott S J 1998 *Chem. Soc. Rev.* **27** 43
- Hall I H, Bastow K F, Warren A E, Barnes C R and Bouet G M 1999 *Appl. Organometal. Chem.* **13** 819
- Lukevics E, Abele R, Fleisher M, Popelis J and Abale E 2003 *J. Mol. Catal. A. Chem.* **198** 89
- Sellman D, Utz J and Heinemann F W 1999 *Inorg. Chem.* **38** 459
- Laranleira M C M, Marusak R A and Lappin A G 2000 *Inorg. Chim. Acta* **186** 300
- Ohta K, Hisaghi R, Kejima M I, Yamamoto I and Kobayashi N 1998 *J. Mater. Chem.* **8** 1979
- Kumar S, Singh R and Singh H 1992 *J. Chem. Soc. Perkin Trans.* **1** 3049
- Muller J G and Takeuchi K J 1990 *Inorg. Chem.* **29** 2185
- Bond A M and Khalifa M 1988 *Aust. J. Chem.* **41** 1389
- (a) Kantouri M L, Papadopolous C D, Quiros M and Hatzidimitriou A G 2006 *Polyhedron* **26** 1292; (b) Srinivasam S, Annaraj J and Athappan P R 2005 *J. Inorg. Biochem.* **99** 876
- Kitiphaisalnont P, Thohinung S, Hanmungtum P, Chaichit N, Patrarakorn S and Siripaisarnpipat S 2006 *Polyhedron* **25** 2710
- Ozer M, Kandaz M, Ozkaya A R, Bulut M and Guney O 2008 *Dyes and Pigments* **76** 125
- Brand U and Vahrenkamp H 1996 *Chem. Ber.* **129** 435
- Zhang Z, Martell A E, Motekaitis R T and Fu L 1999 *Tetrahedron Lett.* **40** 4615
- Earnshaw A 1968 *Introduction to magnetochemistry* (London: Academic Press) p. 4
- Kilic A, Yilmaz I, Ulusoy M and Tas E 2008 *Appl. Organometal. Chem.* **22** 494
- Durmus M, Ahsen V, Luneau D and Pecaut J 2004 *Inorg. Chim. Acta* **357** 588
- Kalinowski H O, Berger S and Braun S 1984 <sup>13</sup>C-NMR-Spektroskopie (New York: Georg Thieme)

22. Gök Y, Kantekin H, Alp H and Ozdemir M 1995 *Z. Anorg. Allg. Chem.* **621** 1237
23. (a) Kumar K N and Ramesh R 2005 *Polyhedron* **24** 1885; (b) Kilic A, Tas E, Gumgum B and Yilmaz I 2006 *Trans. Met. Chem.* **31** 645
24. Ali S A, Soliman A A, Aboaly M M and Ramadan R M 2002 *J. Coord. Chem.* **55** 1161
25. (a) Kandaz M, Koca A and Ozkaya A R 2004 *Polyhedron* **23** 1987; (b) Tas E, Aslanoglu M, Kilic A and Kara Z 2006 *J. Coord. Chem.* **59** 861
26. Rosenthal M R 1973 *T. Chem. Edu.* **50** 331
27. Karapcin F, Dede B, Caglar Y, Hur D, Ilican S, Caglar M and Sahin 2007 *Optics Commun.* **272** 131
28. Kilic A, Tas E, Gumgum B and Yilmaz I 2006 *Chinese J. Chem.* **24** 1599
29. Sacconi L, Ciampolini M, Maffio F and Cavasino F P 1962 *J. Am. Chem. Soc.* **84** 3245
30. Carlin R L 1965 *Trans. Met. Chem.* (New York: Marcel Dekker) vol 1
31. (a) Fraser C and Bosnich B 1994 *Inorg. Chem.* **33** 338; (b) Ilhan S, Temel H, Yilmaz I and Kilic A 2007 *Trans. Met. Chem.* **32** 344
32. (a) Verani C N, Bill E, Renschler E, Weyhermüller T and Chaudhuri P 2000 *J. Chem. Soc. Dalton Trans.* 4263; (b) Tas E, Aslanoglu M, Kilic A and Kara Z 2005 *Trans. Met. Chem.* **30** 758
33. Karabocek S and Karabocek N 1997 *Polyhedron* **16** 1771
34. Cotton F A and Wilkinson G 1988 *Advanced inorganic chemistry* (Wiley-Interscience Publication) 5th edn, p. 725
35. (a) Dutta R L 1981 *Inorganic chemistry* (Calcutta: The New Book Stall) Part II, 2nd edn. p 386; (b) Kilic A, Tas E, Gumgum B and Yilmaz I 2006 *Polish J. Chem.* **80** 1967
36. Srinivasan B R, Dhuri N S, Nathar C and Bensch W 2007 *Trans. Met. Chem.* **32** 64
37. Tas E, Ulusoy M, Guler M and Yilmaz I 2004 *Trans. Met. Chem.* **29** 180
38. Kilic A, Tas E, Gumgum B and Yilmaz I 2006 *Trans. Met. Chem.* **31** 645
39. Kilic A, Tas E, Gumgum B and Yilmaz I 2007 *J. Coord. Chem.* **60** 1233
40. Yilmaz I, Kandaz M, Ozkaya A R and Koca A 2002 *Monatshefte für Chemie* **133** 609
41. Kandaz M, Yilmaz I, Keskin S and Koca A 2002 *Polyhedron* **21** 825
42. Bard A J and Faulkner L R (eds) 2001 *Electrochemical methods: Fundamentals and applications* (New York: John Wiley & Sons) 2nd edn, p. 228
43. Yilmaz I and Kocak M 2004 *Polyhedron* **23** 1279
44. Yilmaz I, Gurek A G and Ahsen V 2005 *Polyhedron* **24** 791
45. Arslan S and Yilmaz I 2006 *Polyhedron* **26** 2387
46. Yilmaz I, Nakanishi T, Gürek A and Kadish M 2003 *J. Porhyr. Phthalocya.* **7** 227